12th AIAA International Space Planes and Hypersonic Systems and Technologies
15 - 19 December 2003, Norfolk, Virginia

AIAA 2003-6924

UPDATE ON MHD CONTROL OF SUPERSONIC / HYPERSONIC BOUNDARY-LAYER TRANSITION

Roger L. Kimmel*

Air Force Research Laboratory

Wright-Patterson AFB, Ohio 45433-7542

Sivaram Gogineni†

Innovative Scientific Solutions, Inc., Dayton, OH 45440

Dayton, OH

Igor Adamovich‡, J. William Rich§

Nonequilibrium Thermodynamics Laboratories

Department Of Mechanical Engineering

The Ohio State University, Columbus, OH 43210

Xiaolin Zhong¶

Mechanical and Aerospace Engineering Department

University of California, Los Angeles, CA 90095

NOMENCLATURE

B =magnetic field, Tesla
$\mathbf{E}$ =electric field vector
$\mathbf{F}$ =Lorentz force vector, Eqn. 1
I =current
K =load factor, E/uB
L =MHD interaction length
M = Mach number
p' =instantaneous pressure
Q =interaction parameter, Eqn. 2.
Re =Reynolds number based on x and boundary-layer edge conditions
T = temperature
U = voltage
u = velocity component in x-direction
x =axial coordinate parallel to model surface cylinder
y = coordinate normal to wall
ρ =density, kg/m^3
σ =plasma conductivity, mho/m

ABSTRACT

The Air Force Research Laboratory, Air Vehicles Directorate, has sponsored computational and experimental research in the control of hypersonic boundary layer transition through a Small Business Innovation Research contract since the year 2000. This work has been presented in several previous papers.[1,2,3] The current paper reviews and summarizes progress in this program and outlines future work.

* Senior Research Engineer, Associate Fellow AIAA
† Senior Engineer, Associate Fellow AIAA
‡ Associate Professor, Associate Fellow AIAA
§ Ralph W. Kurtz Professor, Associate Fellow AIAA
¶ Associate Professor, Associate Fellow AIAA

In Phase I, computational results showed that MHD effects could damp second-mode disturbances that lead to transition in hypersonic boundary layers. Proof-of-concept tests in Phase II showed that wall-pressure fluctuations in a supersonic boundary layer could be damped in an MHD flow, even at relatively low interaction parameter. The second half of the Phase II program focuses on a scaled-up experiment with matching computations.

BACKGROUND

Boundary-layer transition is an important parameter in hypersonic vehicle design. Transition impacts vehicle design primarily through aerodynamic heating, but skin friction drag is important too.[4] Transition also affects pressure drag, engine performance, and aerodynamic control. Estimates for the National Aerospace Plane (NASP)[5] showed that the payload-to-gross-weight ratio would nearly double if the vehicle boundary-layer were fully laminar, compared to fully turbulent.

The impact of boundary layer transition on hypersonic vehicles and the difficulty in predicting it motivates control efforts. Transition is caused by disturbances internal or external to the vehicle. These disturbances engender instabilities in the boundary-layer that amplify and break down into turbulence. At Mach numbers above about five, the second-mode is the primary boundary-layer instability in two-dimensional flows. Any modification of the mean boundary-layer flow or boundary conditions that delays or reduces the instability growth or its initial amplitude can delay transition.

Magnetohydrodynamics (MHD) offers the potential for no-moving-parts flow control. The concept of applying MHD control to hypersonic flows is not new.[6,7] Recent system concepts[8] have renewed interest in this topic, especially concepts including non-equilibrium ionization.

MHD flow control relies on the forces exerted on a conductor (the plasma) flowing through a magnetic field. In the flow shown in Fig 1, plasma flows over a wall with a magnet embedded in it. Assuming a scalar conductivity and negligible electric field, a body force, the Lorentz force, generated on the plasma is given by

$$\mathbf{F} = \sigma(\mathbf{u} \times \mathbf{B}) \times \mathbf{B} \qquad (1)$$

In the vicinity of the magnet pole face, this will be a retarding force, regardless of whether the magnetic field is oriented into or out of the wall, and will distort the mean flow, changing its stability characteristics.

A primary figure of merit for characterizing MHD flows is the interaction parameter, which is the ratio of Lorentz force to inertial forces on a fluid element. For a load factor of unity ($E = UB$), the interaction parameter is

$$Q = \frac{\sigma B^2 L}{\rho u} \qquad (2)$$

The combination of high velocities and low conductivity in hypersonic flows leads to quite low interaction parameters. Compared to liquid metals, for example, the conductivities of plasma airflows are relatively low. The conductivity of liquid mercury is typically cited as 10^6 mho/m.[9] Conductivities of 1-10 mho/m are not unusual for an air plasma.[17] For flight at M=6 at 30km altitude, assuming $\sigma = 1$ mho/m, $L = 1$ meter, and $B = 1$ Tesla (conditions achievable in the laboratory), the interaction parameter based on freestream conditions is Q=0.03, indicating that the fluid inertial forces are quite large compared to the Lorentz force imposed on the fluid.

MHD control of boundary layers would appear to be more promising than control of inviscid flows, and has been considered since at least the 1950's.[10,11] There is no doubt that MHD effects may be used to influence mean boundary-layer profiles,[12,13] which in turn moderate hydrodynamic stability for traveling[11,14] and stationary waves.[15]

The sensitivity of boundary-layer transition to the mean boundary-layer state means that even small MHD control inputs may have a large effect. MHD boundary-layer control exploits the fact that fields from on-board magnets will be highest near the vehicle surface. Also, conductivity, either thermal or non-equilibrium, is highest near the body. If non-equilibrium ionization is employed, the requisite plasma volume is limited. These factors all combine to indicate a potential for MHD flow control with minimum energy requirements.

Despite these benefits, MHD boundary layer control faces significant technical challenges. Ionization is insignificant below about Mach 10 for typical trajectories.[16] Even at reentry velocities, electron number density of the boundary-layer gas is relatively low, leading to low conductivity and low MHD interaction parameter.[17] Non-equilibrium ionization using electric fields or electron-beams, for example, may be used to produce plasma at lower Mach numbers or increase conductivity in thermal plasmas,

but this comes at the price of a weight and energy penalty. Magnet system weight is another drawback. These drawbacks can be mitigated to some extent by identifying the most effective locations for control inputs and limiting their application to these regions.

The interaction parameter may be boosted by imposing an electric field. The Lorentz force on a fluid in the presence of an electric field is

$$\mathbf{F} = \sigma\left(\mathbf{E} + \mathbf{u} \times \mathbf{B}\right) \times \mathbf{B}$$

and the interaction parameter is

$$Q = \frac{\sigma B^2 L}{\rho u} K$$

where K is the load factor, $K = E/uB$. The necessity of boosting the interaction parameter in low-conductivity MHD flows has been recognized and applied for some time to electrolyte flows.[18] Even in hypervelocity flows The load factor may be much larger than one,. For the flow of Ref. 3, E was estimated at 10^4 V/m.

Limited analysis prior to this study supported the concept of stabilizing the boundary-layer to traveling disturbances using MHD forces. Rossow[10] derived velocity profiles for the case of incompressible flow over a flat plate with uniform and non-uniform conductivity in the presence of a transverse magnetic field. As expected, the flow was retarded. Rossow extended these results to calculate the neutral stability diagrams[11] for incompressible flat plate, MHD flows with magnetic fields co-planar and transverse to the mean flow. These results showed a fixed co-planar magnetic field or a transverse field moving with the flow to be stabilizing. A transverse field fixed to the flat plate (generating a retarding force on the mean flow) was destabilizing.

MHD forces affect flow fluctuations as well as the mean flow. For example, if the mean flow is co-planar with the magnetic field and no electric field is imposed, $\mathbf{u} \times \mathbf{B} = 0$ and no Lorentz force is generated due to the mean flow. However, boundary-layer instabilities generate transverse velocity fluctuations, which in turn generate fluctuating Lorentz forces that oppose them. Stuart's[19] calculations for incompressible planar Poiseuille flow of a conducting fluid with a co-planar magnetic field showed that the neutral stability curve shrank with increasing interaction parameter and was completely stabilized with a sufficiently large interaction parameter. Lock's[20] calculations for the same flow with a magnetic field perpendicular to the main flow showed that since this field could operate on the mean flow, it was more effective in stabilizing the flow than the co-planar field.

PHASE I CFD RESULTS

The studies cited above took place before significant computing power was available and before hypersonic boundary layer stability was fully understood. The objective of Phase I of this SBIR was to demonstrate the feasibility of hypersonic MHD transition control computationally. Direct Navier-Stokes Simulation (DNS) was chosen for the computation because Linear Stability Theory (LST) may not apply on the highly nonparallel mean flow distorted by the applied magnetic field. The geometry of the study was rather simple. A Mach 4.5 flow over a two-dimensional flat plate in the presence of an imposed magnetic field was simulated; and all vector components and variations of flow properties in the spanwise direction were neglected. The cold supersonic plasma generated by non-equilibrium ionization was simulated by imposing a uniform 100 mho/m conductivity on the fluid. The imposed magnetic field was generated by two-dimensional magnetic dipoles below the flat plate. The resultant magnetic field is similar to that produced by an array of permanent magnets placed beneath the plate. The governing equations of the MHD flow are formulated from the Navier-Stokes and the Maxwell equations, and were spatially discretized by a fifth-order numerical scheme.

Mach 4.5 flow over a flat plate with two magnetic dipoles of equal strength, one pointing vertically upward and another downward, was considered. The centers of two dipoles are located below the flat plate. The first dipole is located at a distance of 0.02m from the inlet and 0.01m below the plate. Its dipole moment is pointing in the positive *y*-direction. The second dipole is located at a distance of 0.025 m from the inlet, and has the same *y*-location as the first one. The dipole moment of the second dipole is pointing in the negative *y*-direction. For this magnetic dipole arrangement, two cases of different magnetic field strength are considered, a relatively weak B-field of B = 1.2 T at the wall, and a relatively strong field of B = 2.5T at the wall

Numerical results of steady Mach 4.5 weakly ionized flow with a pair of dipoles for both cases are obtained by using the fifth order scheme. The normalized pressure on the wall and the skin friction coefficient are shown in Figs. 2 and 3, respectively. The magnetic dipoles introduce adverse pressure gradient in certain regions but favorable pressure gradients in

other regions. The skin friction coefficient is found to be reduced everywhere on the flat plate for both cases. For the strong magnetic field, there is a local region on the wall where negative skin friction is produced by the magnetic field, indicating a local separation.

Due to the local separation created by the imposed magnetic field, the smooth development of the supersonic boundary layer has been changed. It was natural to expect that the flow would become more unstable, and it is interesting to investigate how the characteristics of the boundary-layer instability modes, especially the second mode, are affected by the magnetic field.

In the computations, the flow was forced at the inlet at the most unstable second-mode frequency. Instantaneous wall-pressure fluctuations shown in Fig. 4 demonstrate that this disturbance is unstable, since the disturbance amplitude increases in the downstream direction. Fig. 5 shows the results of the second mode disturbances in the boundary layer for the weak magnetic field. Compared with the non-MHD results of Fig. 4, the imposed magnetic field has a stabilizing effect on the second mode disturbances. The plots of the instantaneous disturbance of pressure on the wall clearly show that the wave is slightly destabilized in the early zone near the inlet, and then stabilized in the regions where they would be destabilized in the non-MHD case. The disturbance of pressure exhibits a transitional point at about x=0.13m, where the disturbance dies down and gets re-excited before and after that point. The propagation of the second mode wave is substantially damped at x=0.13m, followed by the development of a much weaker wave.

Similar results are found for the stronger magnetic field as shown in Fig. 6. In this case, the stabilization effect on the second mode by the magnetic force is stronger. The second mode wave is significantly stabilized. Although the steady flow in this case has a local separation region (Fig. 3), the second-mode is still stabilized by the magnetic field. This result was somewhat unexpected since one might expect that the separation bubble would greatly destabilize the boundary layer.

One explanation for the strong suppression of the second mode by magnetic forces in a separated flow is the fact the second mode is a trapped acoustic wave reflecting between the wall and a relative sonic layer in the boundary layer. The second mode instability relies only on the existence of a relative supersonic region in the shear layer and does not require the existence of a generalized inflection point. The most-unstable second-mode frequency is strongly tuned to the boundary layer thickness. In the current case of a supersonic boundary layer with an imposed magnetic field, the mean flow boundary layer is substantially altered, greatly thickening the boundary layer thickness, as evidenced by the momentum thickness distributions shown in Fig. 7. Because of this, the wave length of the original growing second mode is no longer tuned with the boundary layer thickness.

PHASE II PROOF-OF-CONCEPT EXPERIMENTS

Although the computations described above were the first to demonstrate stabilization of the second mode using MHD, the actual utility of the concept remained in question. Although the second mode was stabilized, the first mode (corresponding to the Tollmein-Schlichting wave) may be adversely affected by inflectional velocity profiles. The input disturbance in the computation was a 2-D monochromatic wave. In a more realistic flow, lower frequency disturbances tuned to the thicker MHD boundary layer would be present and would be destabilized. Also, the conductivity in an actual, non-equilibrium ionized boundary layer would likely be non-uniform and less than the 100 mho/m conductivity imposed in the computation.

Experiments were carried out to further investigate concept feasibility. Experiments were conducted at the supersonic nonequilibrium plasma wind tunnel facility at the Nonequilibrium Thermodynamics Laboratories of the Ohio State University. This facility generates stable, diffuse supersonic flows of nonequilibrium plasmas at M=2-4, with run durations from tens of seconds to complete steady state [10-12].[21,22,23] A high aspect ratio, rectangular cross section supersonic nozzle made of transparent acrylic plastic is connected to a gas supply system and to a 150 ft^3 ballast tank pumped by a 150 cfm Stokes vacuum pump. The nozzle throat dimensions are 7 mm x 3 mm. To reduce the effect of the side wall boundary layers on the supersonic inviscid core flow, the side walls of the nozzle are slightly diverging at an angle of 1.5°. The nozzle cross section in the test section 10 cm downstream of the throat is 40 mm x 6 mm. During the wind tunnel operation, the static pressure in the test section is monitored using a pressure tap in the nozzle side wall.

Ionization in the supersonic test section (with an electrical conductivity of up to 0.1-1.0 mho/m) is produced by a transverse RF discharge sustained between 24 mm x 5 mm strip copper electrodes

embedded in the nozzle side walls 5 cm downstream of the throat. Both RF electrodes were placed inside C-shaped rectangular quartz or ceramic channels flush-mounted in the walls to prevent secondary electron emission, which would result in the discharge collapse into an arc. The RF electrodes did not extend to the top and bottom nozzle walls to prevent excessive flow heating and hot spot formation in the boundary layers. The RF voltage was applied to the electrodes using an ENI 13.56 MHz, 600 W RF power supply. This sustained a stable, diffuse, and uniform transverse discharge in nitrogen and helium flows.

A 45 MGOe, 1.4 T, 2x2x1 in. Nd-Fe B epoxy coated permanent magnet was flush-mounted in the nozzle side wall 1.5 cm downstream of the RF electrodes as shown in Fig. 8. The magnetic field measured on the magnet surface is 0.45 T (perpendicular to the surface). The magnetic field in the test section can be approximately doubled by placing a second magnet in the opposite nozzle wall. In the present study, a single magnet configuration was preferred since it allowed visual access to the flow. A second nozzle of the same geometry is equipped with a non-magnetized Nd-Fe B block of the same dimensions to provide reference data in the absence of a magnetic field.

The transverse DC electrical current in the supersonic flow pre-ionized by the RF discharge was sustained by applying a DC field (up to ~100 V/cm) to two 50 mm x 5 mm copper electrodes flush mounted in the top and bottom nozzle walls 4 cm apart, perpendicular both to the flow velocity and to the magnetic field direction, as shown in Fig. 8. The estimated reduced electric field does not exceed $E/N \sim 1.0 \cdot 10^{-16}$ V·cm^2, which precludes self-sustained ionization by the DC discharge. In the present measurements, conducted at RF powers of 100-200 W, the DC current density was typically 25 mA/cm^2 at an electric field of 25-50 V/cm, which corresponds to a conductivity of 0.05-0.1 mho/m. The electrical conductivity of the flow can be considerably increased by raising the RF power.

Note that sustaining the transverse DC current using external electric fields has a significant advantage over the current induced by convective motion of electrons in supersonic ionized flows in magnetic fields. Indeed, the drift velocity of electrons in a DC discharge in He at $E/N \sim 1.0 \cdot 10^{-16}$ V·cm^2 reaches ~40 km/sec [13], while the convective flow velocity is only ~1 km/sec. This fact significantly increases the **jxB** force for the same electrical conductivity.

The present measurements were done in helium at a plenum pressure of P_0=1 atm. Helium is chosen primarily because of the slow electron-ion recombination rate which precludes the rapid plasma decay downstream of the RF discharge.[21,22,23] At P_0=1 atm, the steady flow in helium is sustained for about 20 seconds. At a plenum pressure of P=760 Torr, the test section pressure was P_{test}=8.5 Torr, indicating a Mach number of M=3.9. The estimated test section Reynolds number based on the distance from the throat is $Re_x=2.5 \cdot 10^5$.

The pressure fluctuation spectra in the supersonic flows are measured using a miniature microphone located in a plastic tube recessed from the flow by 5 cm. The microphone signal was processed by an HP 35665A dynamic signal analyzer, as shown in Fig. 8. To prevent strong interference with the microphone signal, the RF electrodes were shielded using a grounded brass foil Faraday cage. During each run, the fluctuation spectra taken by the spectrum analyzer were averaged 100 times, which took about a second.

The DC voltage and current were U_{DC}=200 V and I_{DC}=50 mA. This corresponded to a boundary layer magnetic interaction parameter based on the friction velocity of 0.15. At these conditions, the effect of the DC field polarity on the fluctuation spectra was detected. With the cathode on the bottom, which corresponds to a retarding **jxB** force, the fluctuation intensity decreased across the entire frequency range, 100 Hz to 50 kHz, by as much as 50% (see Fig. 9). With cathode on the top (accelerating **jxB** force), there was no detectable effect of the DC field on the fluctuation spectrum in the RF-ionized flow. Note that the DC discharge power, $I_{DC}U_{DC}$ = 10 W, is still a rather small fraction of the RF discharge power, so additional heating of the flow by the DC discharge can be neglected. The test section pressure remained unchanged whether the DC field was on or off, regardless of the polarity.

To verify that the DC field polarity effect is indeed MHD-related, the experiments were repeated in a non-magnetic nozzle for the same conditions as in the second series (RF power 100 W, U_{DC}=300 V, I_{DC}=50 mA). Fig. 10 shows four fluctuation spectra taken at these conditions, again two for each DC field polarity. It can be seen that the spectra are reproduced extremely well and there is no detectable effect of the DC field polarity in the absence of the magnetic field.

A last series of experiments was conducted in a magnetic nozzle in which the magnet was turned 180^0 so that the direction of the magnetic field was now

from the flow into the magnet (i.e. the opposite to the B field direction shown in Fig. 8). In this series, the RF power was 200 W, U_{DC}=100 V, and I_{DC}=50 mA. In this case, the previously observed effect of the pressure fluctuation reduction was reproduced with cathode on top, rather then on bottom (see Fig. 11), which again corresponds to the retarding **jxB** force. It can be seen from Fig. 11 that although the fluctuation intensity reduction effect for the flipped magnet is somewhat weaker than for the original magnet orientation (see Fig. 9), the reproducibility of the results is better.

CONCLUSIONS AND FUTURE PHASE II WORK

Both the computations and experiments indicate the feasibility of damping disturbances in compressible boundary layers using MHD. Although encouraging, both studies were only preliminary in nature, and leave a number of questions unresolved. The experiments provided only limited diagnostics of what was probably a turbulent boundary layer. Also, the damping of disturbances by a decelerating Lorentz force was unexpected. Additional diagnostics in a better-controlled experiment are required to fully diagnose the MHD effects on boundary layers. Also, the experiments were carried out in helium, and need to be extended to air flows.

The objective of Phase II research will be to redress these shortcomings of the Phase I studies. Phase II will feature computations coupled as closely to the experiment as possible. The experiments will be carried out in a new, larger facility with improved magnet and ionization systems, shown schematically in Fig. 12. An aerodynamically contoured M=3 nozzle made of acrylic plastic is connected to a 2 cm x 4 cm rectangular test section 12 cm long. The test section is equipped with three static pressure taps and two Pitot tube ports. Ionization is produced by a transverse RF discharge sustained between two RF electrode blocks 3 cm wide, flush-mounted in the test section walls. Each block, manufactured of high-temperature machinable mica ceramic, incorporates three copper strip electrodes. The RF electrodes are connected to a Dressler 5 kW, 13.56 MHz power supply through an automatic impedance matching network. Very good impedance matching has been achieved, with only about 1-3% of the input RF power reflected back.

The entire nozzle / test section / diffuser assembly can be placed between the poles of a GMW water-cooled electromagnet. In the current configuration fields of up to 1.4T have been achieved.

The transverse DC current in the supersonic flow will be sustained by applying a DC field (up to 10^4 V/m) to two 50 mm x 20 mm DC electrode blocks flush-mounted in the top and bottom nozzle walls 4 cm apart, perpendicular to both the flwo velocity and magnetic field direction. Both continuous and sectioned electrode designs will be tested. The sectioned electrodes allow the application of both transverse and axial DC electric fields in the test section in order to provide a transverse field and cancel the Hall field. The DC field will be applied using a DEL 2 kV / 3A power supply.

Initial tests of the tunnel demonstrate that a stable, combined RF and DC discharge in the presence of the magnetic field can be obtained. Fig. 13 shows a 100 mA DC-discharge in a one-Tesla field

The electromagnet limits optical access to the test section. Schlieren images will be obtained using a mirror system to point the beam through windows on the top and bottom of the tunnel. Optical deflectometry will also be attempted using the windows for access. A 10 mm channel bored in the magnet pole faces will permit spectroscopic measurements using fiber optics.

The computations do not really simulate the true experimental situation, and need to take into account the wind tunnel geometry, the applied electric field, non-uniform conductivity, and the Hall effect. Initial computations are underway to simulate the viscous flow within the new test facility. Flow-field vectors are shown in Fig. 14. Once the non-MHD flow in the facility has been successfully computed, incremental improvements to the code will include the addition of an electric field, non-uniform conductivity, three-dimensionality, and Hall effects

BIBLIOGRAPHY

[1] Cheng, F. Zhong, X., Gogineni, S., Kimmel, R. L., "Effect of Applied Magnetic Field on the Instability of Mach 4.5 Boundary Layer over a Flat Plate, AIAA paper 2002-0351, January 2002.

[2] Palm, P., Meyer, R., Bezant, A., Adamovich, I. V., Rich, J. W., and Gogineni, S, "Feasibility Study of MHD Control of Cold Supersonic Plasma Flows," AIAA paper 2002-0636, January 2002.

[3] Palm, P., Meyer, R., Plönjes, E., Bezant, A., Adamovich, I. V., Rich, J. W., Gogineni, S., "MHD

Effect on a Supersonic Weakly Ionized Flow," AIAA paper 2002-2246, May 2002.
[4] Reed, H. L., Kimmel, R. L., Schneider, S., Arnal, D., and Saric, W., "Drag Prediction and Transition in Hypersonic Flow," AGARD Paper C-15, Symposium on Sustained Hypersonic Flight, AGARD Conference on Future Aerospace Technology in the Service of the Alliance, 14-17 April 1997, Ecole Polytechnique, Palaiseau, France.
[5] Whitehead, A., "NASP Aerodynamics," AIAA paper 89-5013, July 1989.
[6] Kantrowitz, A. R., "A Survey of Physical Phenomena Occurring in Flight at Extreme Speeds," *Proceedings of the Conference on High-Speed Aeronautics*, edited by A. Ferri, N. J. Hoff, and P. A. Libby, Polytechnic Institute of Brooklin, New York, 1955, 335-339.

[7] Resler, E. L., Jr., and Sears, W. R., "The Prospects for Magneto-Aerodynamics," *Journal of the Aeronautical Sciences*, vol. 25, no. 4, April 1958, pp. 235-245, 258.

[8] Gurjanov, E. P. and Harsha, P. T., "AJAX: New Directions in Hypersonic Technology," AIAA Paper 96-4609, November 1996.

[9] Crawford, C. H., and Karniadakis, G. E., "Control of External Flows via Electro-Magnetic Fields," AIAA paper 95-2185, June 1995.
[10] Rossow, V. J., "On Flow of Electrically Conducting Fluids Over a Flat Plate in the Presence of a Transverse Magnetic Field," NACA TN 3971, May 1957.
[11] Rossow, V. J., "Boundary-Layer Stability Diagrams for Electrically Conducting Fluids in the Presence of a Magnetic Field," NACA TN 4282, August, 1958.
[12] Bush, W. B., "Compressible Flat-Plate Boundary-layer Flow With an Applied Magnetic Field," *J. of the Aerospace Sciences*, v. 27, no. 1, Jan 1960, pp. 49-58.
[13] Jaffe, N. A., "Effects of a Transverse Magnetic Field and Spanwise Electric Field on the Boundary-layer of a Conducting Fluid," *AIAA Journal*, vol. 4, no. 10, pp. 1843-1846, Oct. 1966.
[14] Cheng, F. Zhong, X., Gogineni, S., Kimmel, R. L., "Effect of Applied Magnetic Field on the Instability of Mach 4.5 Boundary-layer over a Flat Plate, AIAA paper 2002-0351, January 2002.
[15] Chandrasekhar, S., "The stability of viscous flow between rotating cylinders in the presence of a magnetic field," *Proceedings of the Royal Society of London*, series A, vol. 216, February 1953, pp. 293-309
[16] Bussing, T. R. A., Eberhardt, S., "Chemistry Associated with Hypersonic Vehicles," AIAA paper 87-1292, June 1987.
[17] Sears, W. R. "Magnetohydrodynamic Effects in Aerodynamic Flows," ARS Journal, vol. 29, no. 6, June 1954, pp. 397-406.
[18] Weier, T., Gerbeth, G., Mutschke, G., Platacis, E., Lielausis, O., "Experiments on cylinder wake stabilization in an electrolyte solution by means of electromagnetic forces localized on the cylinder surface," *Experimental Thermal and Fluid Science*, vol. 16, nos. 1&2, January /February 1998, pp. 84-91.
[19] Stuart, J. T., "On the stability of viscous flow between parallel planes in the presence of a co-planar magnetic field," *Proc. Roy. Soc. London*, ser A, vol. 221, no. 1145, 21 Jan 1954.
[20] Lock, R. C., "The stability of the flow of an electrically conducting fluid between parallel planes under a transverse magnetic field," Proc. Roy. Soc. Of London, ser. A, vol. 233, nol. 1192, 6 Dec. 1955, pp. 105-125.
[21] Yano. R., Contini, V., Ploenjes, E., Palm, P., Merriman, S., Aithal, S., Adamovich, I., Lempert. W., Subramaniam. V., and Rich, J.W., "Supersonic Nonequilibrium Plasma Wind Tunnel Measurements of Shock Modification and Flow Visualization", AIAA Journal, vol. 38, No. 10, 2000, pp. 1879-1888.

[22] S. Merriman, E. Plönjes, P. Palm, and I.V. Adamovich "Shock Wave Control by Nonequilibrium Plasmas in Cold Supersonic Gas Flows", AIAA Journal, vol. 39, No. 8, 2001, pp. 1547-1552.

[23] R. Meyer, P. Palm, E. Plönjes, J.W. Rich, and I.V. Adamovich, "The Effect of a Nonequilibrium RF Discharge Plasma on a Conical Shock Wave in a M=2.5 Flow", AIAA Paper 2001-3059.

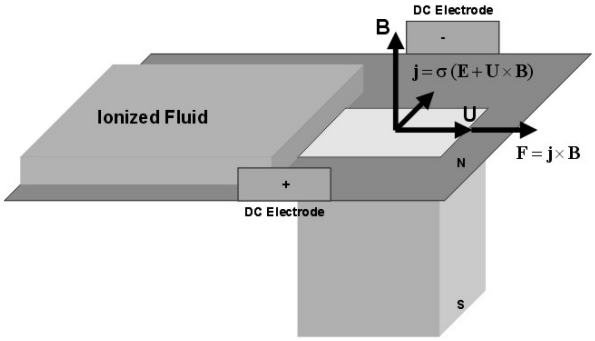

Figure 1 Representation of forces and currents in MHD flow of ionized fluid.

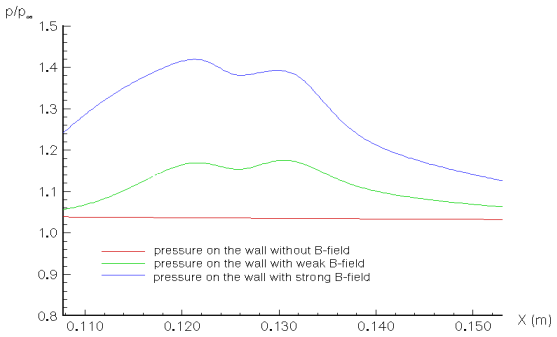

Figure 2 Computed mean surface pressures in MHD flat plate boundary layer.

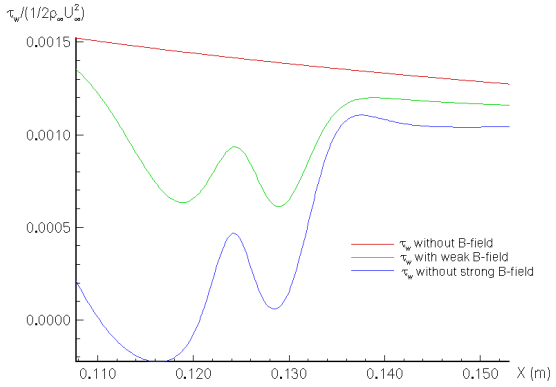

Figure 3 Computed skin friction in MHD flat plate boundary layer.

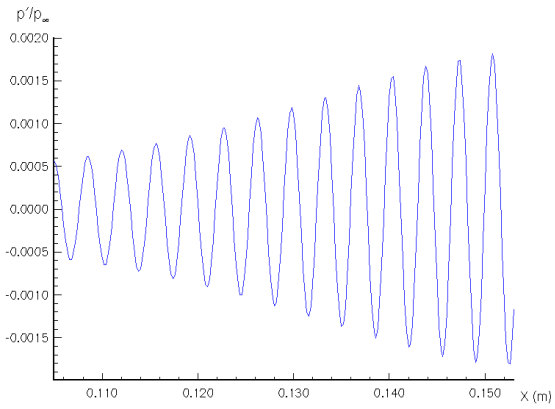

Figure 4 Instantaneous second-mode wall pressure fluctuations in a flat-plate, non-MHD, *M*=4.5 boundary-layer).

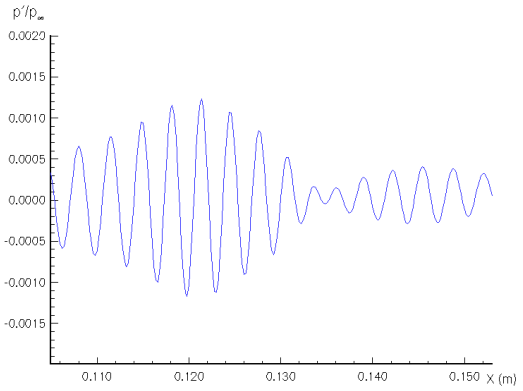

Figure 5 Instantaneous second-mode wall pressure fluctuations in a flat-plate, MHD boundary-layer flow through a 1.2 T field, *M*=4.5.

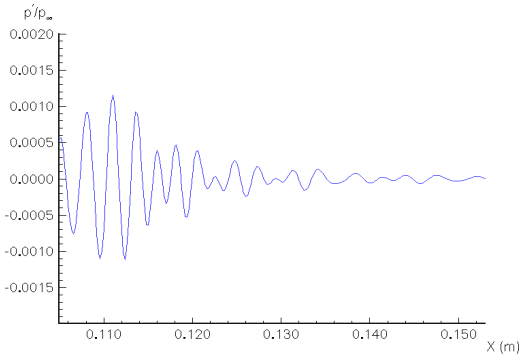

Figure 6 Instantaneous second-mode wall pressure fluctuations in a flat-plate, MHD boundary-layer flow through a 2.5 T field, *M*=4.5.

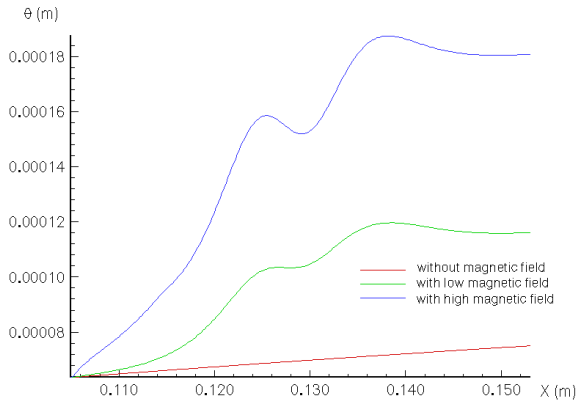

Figure 7 Momentum thickness in MHD flat plate boundary layer.

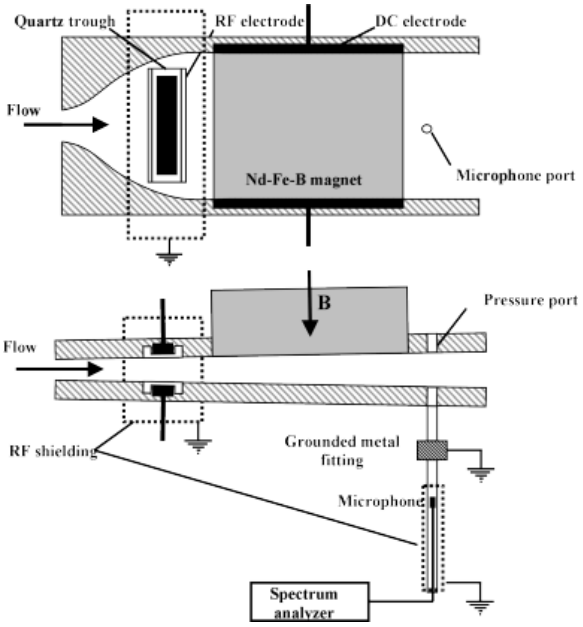

Figure 8 Schematic of MHD test section.

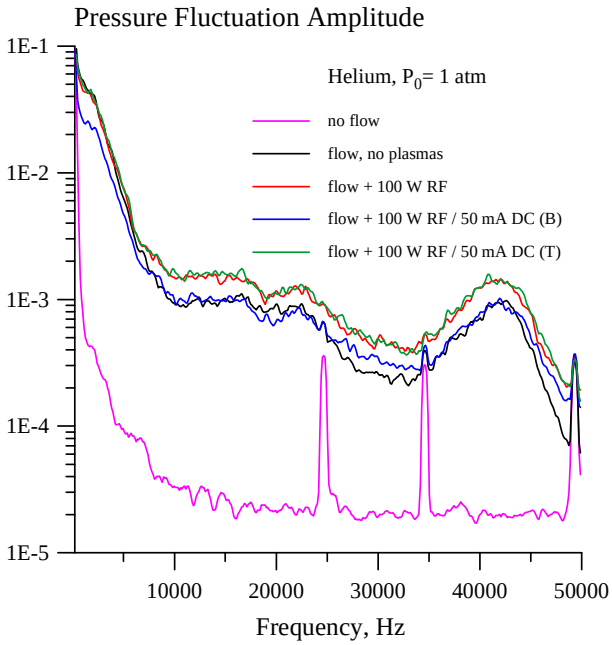

Figure 9 Pressure fluctuation spectra in M=4 helium flows with and without RF and DC discharges at the high DC current. *Magnetic nozzle*, P_0=1 atm, I_{DC}=50 mA. The effect of the DC field polarity is apparent.

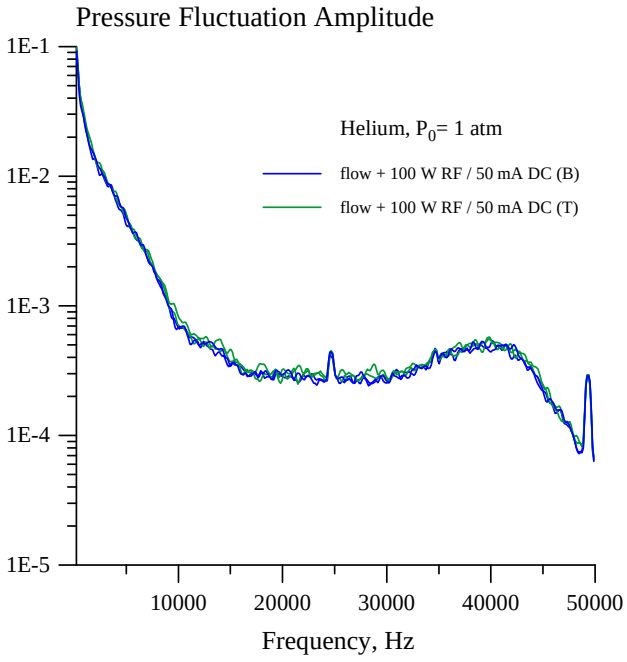

Figure 10 Pressure fluctuation spectra in RF-preionized M=4 helium flows for different DC field polarities. *Non-magnetic nozzle*, P_0=1 atm, I_{DC}=50 mA. Two spectra for each polarity are shown. The effect of the DC field polarity is not detected.

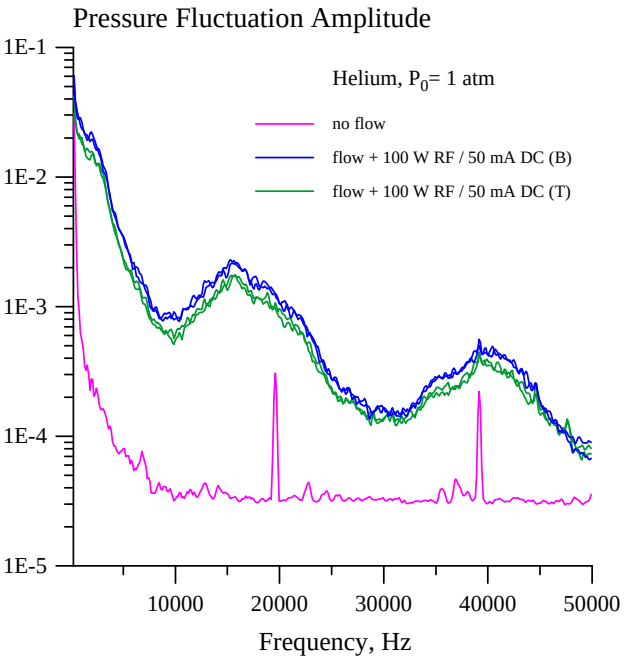

Figure 11 Pressure fluctuation spectra in RF-ionized M=4 helium flows for different DC field polarities. *Nozzle with reversed magnet*, P_0=1 atm, I_{DC}=50 mA. Two spectra for each polarity are shown. The effect of the DC field polarity is now opposite to Fig. 9.

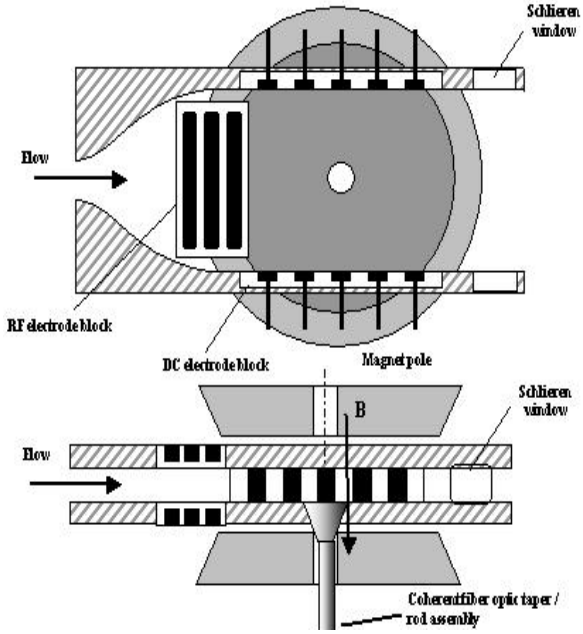

Figure 12 Schematic of new MHD test section.

Figure 13 Image of combined RF-DC discharge in B-field, 100 mA DC at 1 Tesla

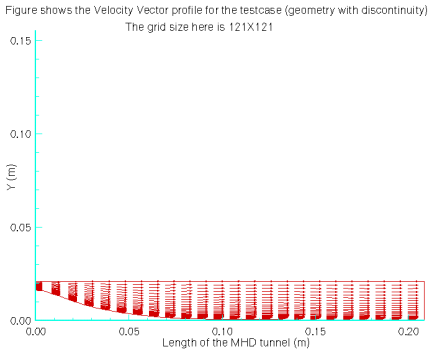

Figure 14 Viscous simulation of flow in new test section.